

Z-scan investigation of fifth-order optical nonlinearity induced by saturable-absorption from (TBA)₂Ni(dmit)₂: application for optical limiting

Chuanlang Zhan,^{*a,b,†} Wei Xu,^a Deqing Zhang,^{*a} Dehuan Li,^b Zhenzhong Lu,^b Yuxin Nie^b and Daoben Zhu^{*a}

^aOrganic Solids Laboratory, Center for Molecular Science, Institute of Chemistry, CAS, Beijing 100080, P.R. China. E-mail: chuanlangzhan@yahoo.com; Tel: 86-10-62529194; E-mail: dqzhang@infoc3.icas.ac.cn; Tel: 86-10-62639355; Fax: 86-10-62559373

^bLaboratory of Optical Physics, Institute of Physics, CAS, Beijing 100080, P.R. China

Received 26th March 2002, Accepted 29th July 2002

First published as an Advance Article on the web 2nd September 2002

The Z-scan technique has been successfully used to determine the magnitudes and signs of the fifth-order optical nonlinearity induced by two-photon absorption. Here, it was used to investigate the fifth-order optical nonlinearity induced by saturable-absorption (SA) of a charge-transfer salt (TBA)₂Ni(dmit)₂ (TBA = tetra-*n*-butylammonium, dmit = 2-thioxo-1,3-dithiole-4,5-dithiolate) with 1064 nm pulses. Under excitation by these 1064 nm pulses, the titled molecule exhibits a typical SA effect at relatively low levels of intensity, while showing strong excited-state absorption (including the first and second excited-state) induced by SA at high intensity levels. Such an excited-state absorption is related to the fifth-order effect. The magnitudes and signs of the fifth- and third-order nonlinearities were estimated. Additionally, the optical limiting effect of this molecule in a dimethyl sulfoxide solution was also studied.

1 Introduction

In the past several years, several papers have been published on Z-scan determination of real and imaginary parts of the fifth-order optical nonlinearity induced by two-photon absorption (2PA) in organic molecules^{1–3} and semiconductors.⁴ The measured values of 2PA-induced excited-state absorptive and refractive cross-sections^{1–4} are in the order of 10^{–18}–10^{–17} cm². Additionally, the second excited-state absorption, which is related to the fifth-order effect induced by reversed-saturable absorption (RSA), has also been observed in cadmium texaphyrin {[T(XP)Cd]Cl}⁵ and 1,3,3,1',3',3'-hexamethylindotri-carbocyanine⁶ by fitting the nonlinear transmittance change as a function of incident intensity. The reported values of the second excited-state absorption cross-section induced by the RSA effect are also in the order of 10^{–18} cm².

As an interesting type of nonlinear optical materials, charge-transfer salts, such as symmetrical and unsymmetrical dithiolenic metal complexes, have been widely investigated^{7–9} because of their high photo-stability to intense irradiation in the near IR region¹⁰ and high nonlinear optical response to the visible and near IR pulses of radiation. The reported values of resonance-enhanced third-order optical nonlinearity, $\chi^{(3)}$, are as high as 10^{–11}–10^{–12} esu.^{7–9} But a fifth-order effect on the total nonlinear absorption and refraction changes of charge-transfer salts is still unknown.

In this article, we report herein Z-scan investigations of the magnitudes and signs of fifth- and third-order optical nonlinearities of a charge-transfer salt, (TBA)₂Ni(dmit)₂, at several high incident intensities using a Q-switched/mode-locked Nd:YAG laser with a duration of 35 ps and a repetition of 10 Hz at 1064 nm. It is observed that this molecule shows typical saturable-absorption (SA) at low incident intensity levels, while exhibiting a strong excited-state absorption

(including the first and second excited-state) induced by SA. This excited-state absorption is related to a fifth-order effect, at high intensity levels.

2 Experimental

2.1 Synthesis

The titled molecule (TBA)₂Ni(dmit)₂ shown in the top of Fig. 1 was synthesized by following a reported procedure¹¹ and purified by crystallization from a mixture of *n*-butanol and acetone in a ratio of 1 : 1. Its purity and chemical structure were confirmed and characterized by ¹H-NMR spectra and elemental analysis. Elemental analysis: Calc. for C₃₈H₇₂N₂S₁₀Ni: C, 48.75; H, 7.75; S, 34.24. Found C, 48.75; H, 7.84; S, 33.73%. Unless stated otherwise, all of the solvents were used as received.

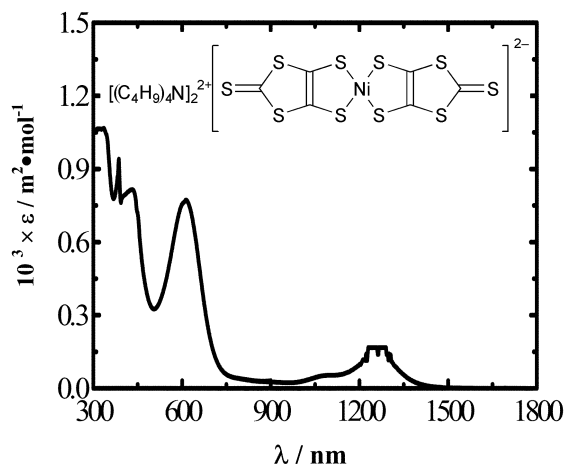


Fig. 1 Linear absorption spectrum of (TBA)₂Ni(dmit)₂ at a concentration of 0.015 M in DMSO. The molecular structure is given above the spectrum.

[†]Present address: Laboratory of Colloid and Interface Science, Center for Molecular Science, Institute of Chemistry, CAS, Beijing, 100080, P.R. China

2.2 Measurements of optical properties

The linear absorption spectrum was measured on a scanning UV-vis-near IR spectrophotometer (Shimadzu UV-3100). In this article, the experimental setup for the Z-scan is similar to that reported in ref. 1. The incident laser beam, which was provided by a Nd:YAG laser with a duration of 35 ps and a repetition rate of 10 Hz at 1064 nm, was focused using an 11 cm focal length lens to give a waist radius $\omega_0 = 20 \mu\text{m}$ (HW1/e²M in irradiance) spot size. An aperture with linear transmittance ($S = 0.18$, here S is the linear transmittance of the aperture used) was placed in the far field for closed-aperture Z-scan measurement. It should be mentioned that surface damage to the liquid cell used was observed as the incident irradiance was larger than 400 GW cm^{-2} . But damage to $(\text{TBA})_2\text{Ni}(\text{dmit})_2$ was not detected because the repeated Z-scan data at low intensity is similar to the initial measured data after the sample was scanned at this maximum intensity (400 GW cm^{-2}). Therefore, all experiments were performed far below this maximum intensity. Z-scan experiments were performed with a 0.2 mm pathlength glass liquid cell containing a 0.015 M solution of $(\text{TBA})_2\text{Ni}(\text{dmit})_2$ in dimethyl sulfoxide (DMSO). The linear transmittance of this 0.015 M solution in the 0.2 mm pathlength glass liquid cell is 86%, and the linear absorption coefficient (α) was calculated to be 7.3 cm^{-1} . Accordingly, the ground state absorption cross-section (σ_0) was estimated to be $8.1 \times 10^{-19} \text{ cm}^2$ using the equation $\alpha_0 = 10^{-3} N_A \sigma_0 d_0$, where N_A is the Avogadro number and d_0 is the concentration of the sample (in units of mol l^{-1}).

3 Results and discussion

Fig. 1 shows the linear absorption spectrum in the range from 300 to 1800 nm of a 0.015 M solution of $(\text{TBA})_2\text{Ni}(\text{dmit})_2$ in DMSO. The contributions to the spectrum of the liquid cell and solvent (DMSO) were subtracted. Obviously, this solution shows a strong linear absorption band with peaks at 613, 431, 335, and $\sim 320 \text{ nm}$ in the UV-vis region. Interestingly, it also exhibits a relatively weak absorption band with two peaks at about 1246 and 1277 nm in the near IR region (900 to 1600 nm). These near IR transitions may be assigned to the $\pi \rightarrow \pi^*$ transition.¹²

As reported in refs. 1–4, both nonlinear absorption and nonlinear refraction of the titled molecule induced by intense laser radiation can be separately measured with open and closed Z-scan experiments respectively at several incident intensities. Fig. 2 shows six open-aperture Z-scans for the

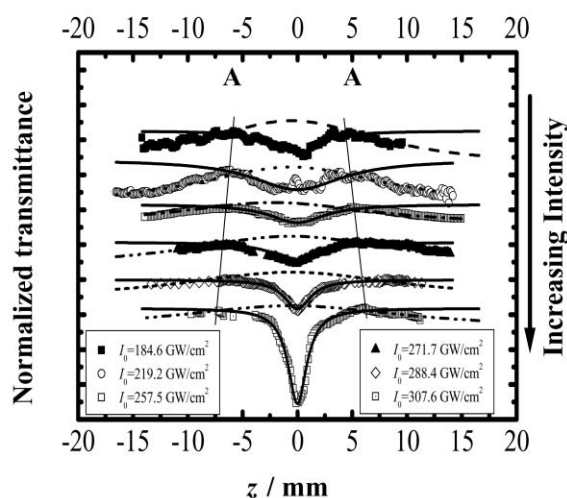


Fig. 2 A typical series of open-aperture Z-scans at several incident intensities from $184.6\text{--}307.6 \text{ GW cm}^{-2}$. The dashed and solid curves are the best fitted lines through eqns. (1) and (2), respectively.

$(\text{TBA})_2\text{Ni}(\text{dmit})_2$ solution at six peak-on-axis input irradiances (I_0) from 184.6 to 307.6 GW cm^{-2} . Here $I_0 = 4(\ln 2)^{1/2} E_{\text{total}} / (\pi^3)^{1/2} \omega_0^2 \tau_L$, where E_{total} is the incident energy on the sample after reflection from the front surface of the glass cell and solvent has been subtracted, and τ_L is the pulse duration. It is seen in Fig. 2 that the open-aperture Z-scan at low intensity levels shows a typical SA configuration in the region far from the focus and a SA-induced first excited-state absorption (e.g. $S_1 \rightarrow S_2$) near the focus. In other words, the normalized transmittance increases initially as the sample is moved towards the focus of the laser beam from the far field, and then decreases after the maximum is reached at point A (see Fig. 2). The decrease in transmittance near the focus suggests the first excited-state absorption contributes to the total nonlinear absorption change. As expected, point A (see Fig. 2) moves further from the focus as the incident intensity increases from 184.6 to 307.6 GW cm^{-2} . The ordinate (e.g. normalized transmittance, named as T_{int}) of point A is the same for each open-aperture Z-scan; $T_{\text{int}} = 1.06 T_{\text{int}}$, where T_{int} is the initial linear transmittance at $I_0 = 0$. From this equation, T_{int} is calculated to be 91.2% based on $T_{\text{int}} = 86\%$. Of particular interest, the excited-state absorption effect becomes much stronger when the incident intensity increases up to 307.6 GW cm^{-2} . This fact implies that there could be another reason for the drop of normalized transmittance near the focus from a higher excited-state, such as the second excited-state absorption (e.g. $S_2 \rightarrow S_n$), which is related to a fifth-order effect. Such second excited-state absorption contributions to nonlinear absorptions were also observed in $\{[(\text{TXP})\text{Cd}]\text{Cl}\}^5$ and 1,3,3,1',3',3'-hexamethylindotricarbocyanine.⁶

Now we turn to estimate the excited-state absorption cross-section. If the contributions from the excited-states absorptions ($S_1 \rightarrow S_2$ and $S_2 \rightarrow S_n$) are ignored, the lifetime (τ_1) of the S_1 state can be estimated by eqn. (1),

$$T = \exp \left[-\alpha_0 L_{\text{eff}} \left(\frac{1}{1 + I_0 / I_{\text{sat}}} \right) \right] \quad (1)$$

where $I_{\text{sat}} = hv / (\sigma_0 \tau_1)$ is the saturable intensity, hv is the photon energy of the pulse laser used in this work, and $L_{\text{eff}} = [1 - \exp(-\alpha L)] / \alpha$ is the effective pathlength, with L the pathlength of the liquid cell ($L = 0.2 \text{ mm}$ in this work), to be on average 0.43 ns^{13} by fitting the six open-aperture Z-scan data in the SA region.

But, in the region near the focus where an obvious RSA occurs, on the basis of the following two approximations, the data can be fitted by eqn. (2),¹⁴

$$T = \frac{\ln \left(1 + \frac{q_0}{1+x^2} \right)}{q_0 / (1+x^2)} \quad (2)$$

where $q_0 = \alpha' \sigma_{\text{ex}}^{\text{eff}} F_0(r=0) L_{\text{eff}} / 2hv$, with $F_0 = 2E_{\text{total}} / \pi \omega_0^2$ the peak-on-axis fluence, and $x = z / Z_0$, with z the position of the sample from the focus, $Z_0 = \pi \omega_0^2 / \lambda$ the Rayleigh range and λ the wavelength of the laser pulse used ($\lambda = 1064 \text{ nm}$ in the present case). One approximation is that the contribution to the total nonlinear absorption change from the second excited-state absorption is assumed to be involved in that from the first excited-state absorption to yield an effective excited-state absorption cross-section ($\sigma_{\text{ex}}^{\text{eff}}$), which can be used in eq (2). The other is that, the linear absorption coefficient α' used in eq (2) is related to T_{int} , e.g. the ordinate of point A (Fig. 2) at which the RSA effect occurs. On the basis that $T_{\text{int}} = 1.06 T_{\text{int}}$ and $\alpha = 7.3 \text{ cm}^{-1}$, the linear absorption coefficient α' at point A is calculated to be 4.6 cm^{-1} .

Fig. 3 shows a plot of $\sigma_{\text{ex}}^{\text{eff}}$ obtained from the six open-aperture Z-scans by eqn. (2) versus I_0 . Apparently, the $\sigma_{\text{ex}}^{\text{eff}}$ shows a slight decrease with I_0 at low intensity levels, while exhibiting a large increase with I_0 at high intensity levels. The initial decrease in $\sigma_{\text{ex}}^{\text{eff}}$ indicates that an aggregated effect

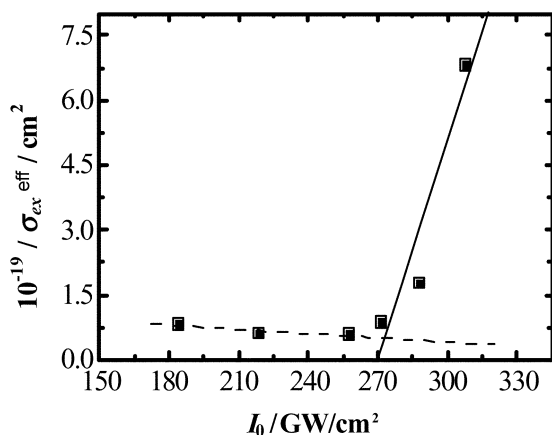


Fig. 3 Plots of effective excited-state absorption cross-section, $\sigma_{\text{ex}}^{\text{eff}}$, versus I_0 . The initial decrease of $\sigma_{\text{ex}}^{\text{eff}}$ at low intensity levels indicates that an aggregated effect occurs, while the dramatic increase at high intensity levels suggests that a fifth-order effect such as a second excited-state absorption occurs.

occurs, as is observed for some stilbazolium derivatives.^{1,2} Linear fits of these data at low intensity levels yields an intercept, *e.g.* the first excited-state absorption cross-section, as $\sigma_1 = 1.38 (\pm 0.14) \times 10^{-19} \text{ cm}^2$, from which both the aggregation and higher excited-state absorption effects such as the second excited-state absorption have been subtracted.^{1,2} The ratio of σ_1 and σ_g (where σ_g is the ground state cross-section) indicates that the titled molecule exhibits typical saturable-absorption. The dramatic increase at high intensity levels suggests that a fifth-order effect, such as the second excited-state absorption, occurs. Best fitting of the data at high incident intensity levels in Fig. 3 yields a slope ($C = 1.68 (\pm 0.17) \times 10^{-20} \text{ cm}^4 \text{ GW}^{-1}$), from which the second excited-state absorption cross-section (σ_2), *e.g.* the fifth-order nonlinear absorptive cross-section, can be estimated to be $5.5 (\pm 0.55) \times 10^{-18} \text{ cm}^2$ from $C = (0.12\sigma_1\sigma_2\tau_1/h\nu)$.¹⁵ It should be noted that the value of σ_2 , which is in the order of 10^{-18} cm^2 , is similar to those reported in refs. (5) and (6). Comparison of σ_0 , σ_1 and σ_2 values indicates that $\sigma_2 > \sigma_0 > \sigma_1$, suggesting that the titled molecule possesses a strong second excited-state absorption rather than the ground and first excited-state absorptions. Thus, it is reasonable for a typical RSA process to occur near the focus.

The imaginary part of the third-order optical nonlinearity can be estimated to be $-0.21 (\pm 0.02) \times 10^{-12} \text{ esu}$ from eqn. (3),¹⁶

$$\chi^{(3)}_{\text{Im}}(\text{esu}) = (-cn_0^2/32\pi^2)(c\alpha/\omega I_{\text{sat}})(\text{MKS}) \quad (3)$$

where c is the speed of light in meters per second and n_0 is the linear refractive index of solvent ($n_0 = 1.48$ for DMSO).

The closed-aperture and divided Z-scans shown in Fig. 4 exhibit an obvious peak–valley signature. A similar signature was also observed for five other closed-aperture and divided Z-scans at five other input irradiances. In principle, such a nonlinear refraction can be due to the solute, solvent or glass liquid cell. Measurements of both open- and closed-aperture Z-scans of only the solvent and glass liquid cell indicates that only a positive nonlinear refraction signal was observed, while no obvious nonlinear absorption signal was detected. In addition, a higher-order effect on the nonlinear refraction of the solvent and glass liquid cell was also not detected. These facts indicate that $(\text{TBA})_2\text{Ni}(\text{dmit})_2$ exhibits a negative total nonlinear refraction.

The nonlinear transmittance difference of the peak–valley, ΔT_{p-v} , was estimated to be 0.10 for all the six divided Z-scans at six incident irradiances. On the basis of the known value of

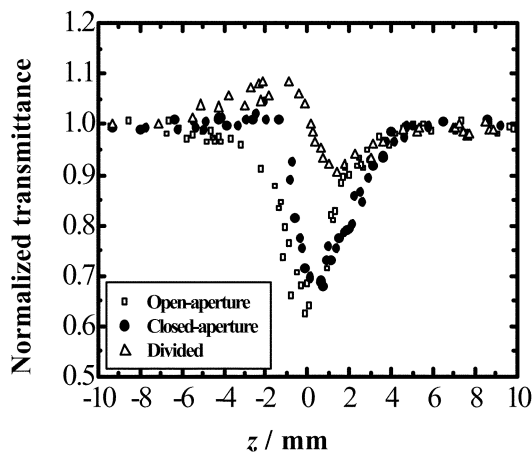


Fig. 4 A typical series of open-aperture (filled-squares), closed-aperture (filled-circles), and divided (filled-uptriangles) Z-scans at a fixed incident intensity of $315.1 \text{ GW cm}^{\delta 2}$.

ΔT_{p-v} , the nonlinear refraction change Δn can be calculated according to the eqn. (4),^{3,4}

$$\Delta n/I_0 = \Delta T_{p-v} / [0.406(1-s)^{0.25}kL_{\text{eff}}I_0] = n_2 + B\sigma_r I_0 \quad (4)$$

where $k = 2\pi/\lambda$, σ_r is the fifth-order refractive cross-section and B is a constant. In general, at low input irradiance, Δn is attributed mainly to the third-order contribution, but at high input intensity, it may also be contributed to by a higher-order effect.

The plot of $\Delta n/I_0$ versus I_0 shown in Fig. 5 indicates that $\Delta n/I_0$ increases with increasing intensity. Linear fitting of the data gives a straight line with a positive slope $C' = 5.8 (\pm 0.6) \times 10^{-9} \text{ cm}^4 \text{ GW}^{-2}$ and a negative intercept $n_2 = -6.0 (\pm 0.6) \times 10^{-6} \text{ cm}^2 \text{ GW}^{-1}$. The value of n_2 is in agreement with the reported values for other symmetrical dithiolenic metal complexes (in the order of $10^{-5} \text{ cm}^2 \text{ GW}^{-1}$).⁸ This negative intercept and positive slope show that $(\text{TBA})_2\text{Ni}(\text{dmit})_2$ exhibits negative third- and positive fifth-order contributions to nonlinear refraction, and the third-order effect is larger than that of fifth-order. Thus, a negative signature in divided Z-scans was observed. Additionally, nearly the same value of ΔT_{p-v} was also observed with increasing I_0 . The negative third-order nonlinear refractive index of n_2 can be attributed to the bound electrons, while the positive fifth-order effect on nonlinear refraction may be due to a change in n_2 caused by the production of SA-generated excited-states.³ The value of n_2 was obtained as $-2.1 (\pm 0.2) \times 10^{-12} \text{ esu}$ from the negative intercept from $n_2 (\text{esu}) = (cn_0/40\pi)n_2 (\text{MKS; metre, kilometre,}$

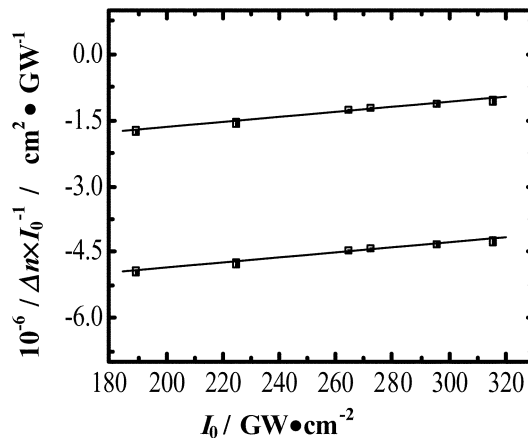


Fig. 5 Plot of $\Delta n/I_0$ versus I_0 . The positive slope and negative intercept reveal that this molecule shows positive fifth-order and negative third-order contributions to the nonlinear refraction effect.

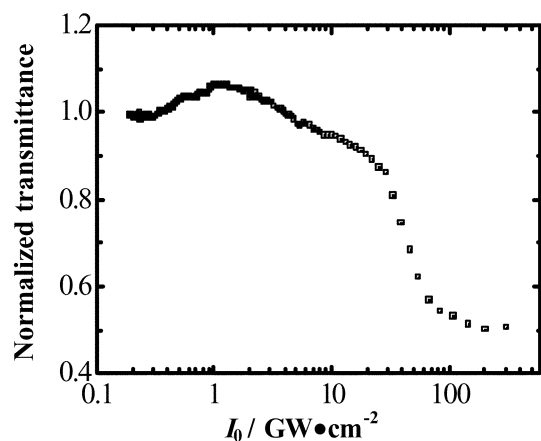


Fig. 6 The characteristic nonlinear transmittance as a function of incident intensity. The initial increase of normalized transmittance at low intensity levels indicates a typical saturable absorption, while the dramatic decrease at high intensity levels shows a typical reversed-saturable absorption.

second).¹⁴ The real part of the third-order optical nonlinearity $\chi_{\text{Re}}^{(3)}$ can be calculated as $-7.9 (\pm 0.8) \times 10^{-12}$ esu from eqn. (5).¹⁴

$$\chi_{\text{Re}}^{(3)}(\text{esu}) = (cn_0^2/16\pi^2)n^2(\text{MKS}) \quad (5)$$

This value is larger than that of $\chi_{\text{Im}}^{(3)}$, indicating that third-order nonlinear refraction dominates the third-order optical nonlinearity. It is also worth noting that the value of $\chi_{\text{Re}}^{(3)}$ also coincides with those reported in refs. 7–9. The real part of the fifth-order optical nonlinearity, e.g. the fifth-order refractive cross-section, σ_r , can be calculated as 3.00×10^{-19} cm² from $C = (0.23\alpha\sigma_1\sigma_r\tau_L^2/k(h\nu)^2)$.¹⁵ Comparison of σ_2 and σ_r indicates that the titled molecule shows strong fifth-order nonlinear absorption rather than refraction.

The open-aperture Z-scans shown in Fig. 2 indicates that a solution of the titled molecule exhibits an obvious change in the normalized transmittance near the focus, especially for open-aperture Z-scans at high intensity levels. This fact reveals that (TBA)₂Ni(dmit)₂ is an interesting candidate for optical limiting effects.

Fig. 6 shows the characteristic optical limiting performance obtained from open-aperture Z-scan data; it is seen that the normalized transmittance (T) shows an initial increase at low intensity levels. After reaching a maximum, it then decreases slowly. This fact confirms a typical saturable-absorption effect and the contribution of the first excited-state absorption. When I_0 increases up to about 25 GW cm⁻², a dramatic decrease in the normalized transmittance to about 0.5 is observed, indicating that a strong second excited-state absorption occurs. When $I_0 > 100$ GW cm⁻², the normalized transmittance then decreases slowly to a plateau, suggesting that the strong excited-state absorption is still active.

4 Conclusions

The magnitudes and signs of both the fifth- and third-order optical nonlinearities of (TBA)₂Ni(dmit)₂ in solution were

determined by the Z-scan technique using a picosecond pulse laser at 1064 nm. Experimental results indicate that (TBA)₂-Ni(dmit)₂ exhibits both relatively weak saturable-absorption and strong third-order refraction, while showing strong excited-state absorption induced by this saturable-absorption effect and weak fifth-order nonlinear refraction. The second excited-state absorption e.g. the fifth-order nonlinear absorptive cross-section was estimated to be in the order of 10^{-18} cm², while the fifth-order nonlinear refractive cross-section is about 10^{-19} cm².

Acknowledgements

The authors would like to thank Bao-Hua Feng, Xiu-Lan Zhang and Li-Zeng Zhao for help with the experiment setup. The present work was supported financially by the Chinese Academy of Sciences and the State Key Basic Program. This work was also supported by the Foundation of the Laboratory of Optical Physics, Institute of Physics, The Chinese Academy of Sciences.

References and notes

- C. L. Zhan, D. Q. Zhang, D. B. Zhu, D. Y. Wang, Y. J. Li, D. H. Li, Z. Z. Lu, L. Z. Zhao and Y. X. Nie, *J. Opt. Soc. Am. B*, 2002, **19**, 369.
- C. L. Zhan, D. H. Li, D. Y. Wang, D. Q. Zhang, Y. J. Li, Z. Z. Lu, L. Z. Zhao, Y. X. Nie and D. B. Zhu, *Chem. Phys. Lett.*, 2001, **347**, 410.
- A. A. Said, C. Wamsley, D. J. Hagan, E. W. Van Stryland, B. A. Reinhardt, Paul Roderer and Ann. G. Dillard, *Chem. Phys. Lett.*, 1994, **228**, 646.
- A. A. Said, M. Sheik-Bahae, D. J. Hagan, T. H. Wei, J. Wang, J. Young and E. W. Van Stryland, *J. Opt. Soc. Am. B*, 1992, **9**, 405.
- J. H. Shi, M. Yang, Y. X. Wang, L. Zhang, C. F. Li, D. Y. Wang, S. M. Dong and W. F. Sun, *Appl. Phys. Lett.*, 1994, **64**, 3063.
- S. Hughes, G. Spruce, B. S. Wherrett, K. R. Welford and A. D. Lord, *Opt. Commun.*, 1993, **100**, 113.
- C. S. Winter, C. A. S. Hill and A. E. Underhill, *Appl. Phys. Lett.*, 1991, **58**, 107.
- C. A. S. Hill, A. Charlton, A. E. Underhill, K. M. Abdul-Malik, M. B. Hursthouse, A. I. Karaulov, S. N. Oliver and S. V. Kershaw, *J. Chem. Soc., Dalton. Trans.*, 1995, 587.
- J. Dai, G. Q. Bian, X. Wang, Q. F. Xu, M. F. Zhou, M. Munakaa, M. Maekawa, M. H. Tong, Z. R. Sun and H. P. Zeng, *J. Am. Chem. Soc.*, 2000, **122**, 11007.
- U. T. Mueller-Weserhoff, B. Vance and D. I. Yoon, *Tetrahedron*, 1991, **47**, 909.
- A. Kobayashi, H. Kim, Y. Sasaki, R. Kato, H. Kobayashi, S. Moriyama, Y. Nishio, K. Kajita and W. Sasaki, *Chem. Lett.*, 1987, 1819.
- Z. S. Herman, B. F. Kirchner, G. H. Loew, U. T. Mueller-Westerhoff, A. Nazzal and M. C. Zerner, *Inorg. Chem.*, 1982, **21**, 46.
- M. Samoc, A. Samoc, B. Luther-Davies, H. Reisch and U. Scherf, *Opt. Lett.*, 1998, **23**, 1295.
- W. F. Sun, M. M. McKerns, C. M. Lawson, G. M. Gray, C. L. Zhan and D. Y. Wang, *Proc. SPIE*, 2000, **4106**, 280.
- The two equations of $C = (0.12\sigma_1\sigma_2\tau_L/h\nu)$ and $C' = (0.23\alpha\sigma_1\sigma_r\tau_L^2/k(h\nu)^2)$ were deduced by using a similar process to that described in refs. 3 and 4.
- L. Yang, R. Dorsinville, Q. Z. Wang, P. X. Ye and R. R. Alfano, *Opt. Lett.*, 1992, **17**, 323.